A Proposal for a New, Simplified Methodology for Design Flow Modeling in Ungauged Catchments

DARIUSZ MŁYŃSKI,[a] DEVENDRA M. AMATYA,[b] ANDREA PETROSELLI,[c] ANDRZEJ WAŁĘGA,[a] AND SOURAV MUKHERJEE[b]

[a] *Department of Engineering Sanitary and Water Management, University of Agriculture in Krakow, Krakow, Poland*
[b] *Center for Forest Watershed Research, Southern Research Station, USDA Forest Service, Cordesville, South Carolina*
[c] *Department of Agriculture and Forest Sciences (DAFNE), Tuscia University, Viterbo, Italy*

(Manuscript received 24 March 2024, in final form 15 February 2025, accepted 3 March 2025)

ABSTRACT: The primary objective of this research was to propose a new methodology for calculating design flows in ungauged catchments, addressing uncertainties associated with outdated empirical formulas. Focusing on four catchments in the eastern United States, the methodology comprises two main steps: 1) determination of peak flow series using the Event-Based Approach for Small Ungauged Basins (EBA4SUB) rainfall–runoff model and 2) calculation of design flows based on the generated series from EBA4SUB, utilizing the best-fitted statistical distribution. Linear scaling was applied to reduce the percent bias (PBIAS) error in design flows. The study encompassed trend analysis for hydrometeorological data, estimation of peak flow series using EBA4SUB, and the calculation of design flows with the proposed methodology. Validation involved comparing estimated design flows from observed time series with those calculated via the Graphical Peak Discharge (GPD) method and the Rational Formula. Results indicated no significant ($\alpha = 0.05$) trends in peak flow series and identified the Pearson type III distribution as best fitted for design flows. Hydrological modeling underscored the critical role of antecedent-moisture conditions in calculating design flows. The calculated PBIAS values of <10% for model validation suggest the proposed methodology is suitable for use in ungauged catchments.

SIGNIFICANCE STATEMENT: Design flows are pivotal in environmental management for several reasons. First, they aid in planning water infrastructure with minimal environmental impact. Second, they inform flood protection strategies vital for safety and property protection. Understanding design flows is crucial for safeguarding aquatic ecosystems and determining minimum flows for a healthy environment. They are also vital in managing water-related risks such as floods, particularly amid climate change. Currently, estimating design flows in ungauged catchments relies heavily on multivariate correlation analysis, which may be outdated due to climate changes and land-use alterations. Our research proposes a novel methodology using the Event-Based Approach for Small Ungauged Basins (EBA4SUB) rainfall–runoff model and statistical distributions to calculate design flows in ungauged catchments to address these concerns.

KEYWORDS: North America; Extreme events; Statistical techniques; Hydrologic models; Annual variations

1. Introduction

Catchments are complex and heterogeneous systems consisting of a wide range of natural or anthropogenic processes and, thereby, are characterized by considerable spatial and temporal variability of hydrological processes. This is evidenced by the interaction between topography, geomorphology, and geological factors, coupled with climatological characteristics that make the hydrological responses highly complex (Liu et al. 2021). Full understanding of these processes plays a crucial role to quantitatively manage runoff, especially specific to flood events. It becomes even more important in cases when climate or land use and land cover are continuously changing.

One of the main hydrological characteristics used for flood protection is design flows. The method of determining them depends on whether a given watershed is gauged or ungauged. In the case of gauged catchments, the design flows are determined based on the statistical distribution of random variables. However, recent years have seen a decreasing trend in available gauged catchments that provide continuous hydrological information. This is primarily associated with the costs of maintaining such monitoring stations (Bezak et al. 2016; Bhagat 2017). In the case of ungauged catchments, design flows can be determined based on multiple correlation equations, regional frequency analysis, or by applying rainfall–runoff hydrological models. Empirical formulas, however, have many limitations inherent in their construction. Therefore, rainfall–runoff hydrological models are often used to determine design flows. In particular, most practitioners mainly utilize event-based models. This is because the structure and operation of these models are relatively simplified, making them easy to use (Berthet et al. 2009). Recently, hydrological modeling based on continuous simulations is increasingly being used. Continuous models precisely reflect hydrological processes, particularly tracking the soil moisture. However, they are based on a larger number of input parameters, making them more challenging to calibrate. Additionally, some studies have shown that results obtained from event-based

Corresponding author: Dariusz Młyński, dariusz.mlynski@urk.edu.pl

DOI: 10.1175/JHM-D-24-0037.1

models are comparable to continuous simulation models. Petroselli et al. (2019b) demonstrated that the difference for design flows with a return period of 100 years between these two types of models is only 7%. Hossain et al. (2019) showed that in some cases, event-based simulations can yield better results than continuous simulations. Additionally, the limitations of models pose challenges in selecting the optimal rainfall simulation model for specific risk analysis needs. Due to this, event-based models are finding widespread use in flood prediction and design flows estimation including in forested catchments (Mukherjee et al. 2025; Amatya et al., 2021a). They concentrate on specific rainfall events and their influence on the catchment response. These models prove beneficial in regions where continuous hydrological data might be lacking or less reliable. On the other hand, continuous simulation models are valuable for extended water resources planning, management, and evaluating the impact of land use and climate change over the long term (Kemp and Alankarage 2023; Mukherjee et al. 2025).

Among several event-based rainfall–runoff models available in the literature, the most common are conceptual models based on the Nash cascade of linear reservoirs, geomorphological laws of a river network, or synthetic unit hydrographs, such as the Snyder model or Soil Conservation Service-Unit Hydrograph (SCS-UH) (Młyński et al. 2018). However, experience with such models has shown some limitations. For example, these models are highly sensitive to the design hyetograph, unreliable estimation of net rainfall, and the subjectivity of choosing the values of some indicators for estimating model parameters. These limitations often yield high uncertainties in flood magnitudes. Therefore, a sensitivity analysis and model calibration are fundamental for evaluating the model's performance and helping in a better understanding of the simulated flood processes (Wałęga 2016; Młyński 2020).

An advancement in commonly used empirical–conceptual rainfall–runoff models is the Event-Based Approach for Small Ungauged Basins (EBA4SUB) developed by Grimaldi and Petroselli (2015). It includes a series of modules, which are typically designed for event-based procedures: design rainfall estimation, design hyetograph elaboration, net rainfall estimation, and rainfall–runoff transformation. The EBA4SUB model needs a limited number of input data such as a design hyetograph, digital elevation model (DEM), and information about soil property and land use (Piscopia et al. 2015). In the model, the net rainfall is calculated using the curve number (CN) procedure (USDA 1986) in the Green–Ampt equation (Green and Ampt 1911), referred to as CN for Green–Ampt (CN4GA) (Grimaldi et al. 2013). Rainfall to runoff transformation is achieved using a particular version of the instantaneous unit hydrograph based on the width function (Grimaldi et al. 2012a). In the literature, EBA4SUB was tested in several catchments, and the model outputs were compared with observed runoff and showed good agreement. An example is the research conducted by Vojtek et al. (2019), who tested the EBA4SUB model in terms of its use for flood inundation mapping in a small (with an area of about 25 km^2) upland-agricultural catchment.

Taking into consideration the issues related to determining design flows in ungauged catchments as well as the limitations concerning the application of rainfall–runoff models in forested catchments, the main aim of the study was to propose a new approach for estimating design flows in forested catchments. The method is based on two stages. The first involves designation of peak flow series using the EBA4SUB model. The second is design flow estimation through statistical distributions, based on the generated series of peak flows. The proposed methodology is an original solution, being applied for the first time in forested catchments, which constitutes a novelty in the conducted research. At the same time, it should be emphasized that this approach is universal and can be applied in watersheds with different land-use characteristics. The obtained results were compared with other methods for estimating design flows, such as the Rational Formula (RF) and the Graphical Peak Discharge (GPD). The research was conducted for headwater catchments managed by the U.S. Department of Agriculture Forest Service (USDA-FS) as was recently reported elsewhere (Amatya 2021b; Mukherjee et al. 2024).

2. Study area

The USDA-FS manages four experimental forested catchments in the southeastern United States: WS80 and WS78, situated at the Santee Experimental Forest in South Carolina (SC); WS14, located within the Coweeta Hydrological Laboratory in North Carolina (NC); and WS3, part of the Hubbard Brook Experimental Forest in New Hampshire (NH). Figure 1 presents the geographical location, boundary, and stream channels for each of the four catchments analyzed in the study. Their main characteristics such as drainage area A, length of main channel L, average slope of catchment S, and slope of main channel I are listed in Table 1.

The specific catchments were selected for analysis to incorporate the synoptic climate, morphological, and topographic variability within the United States. For example, WS78 and WS80 are located at the Santee Experimental Forest in South Carolina, which has a humid subtropical climate and lowland topography. The soils in this area are predominantly Aquic Alfisols and Ultisols—somewhat poorly to poorly drained sandy loams with clayey subsoils. These soils have high surface-water retention capacity and low permeability, resulting in slow surface-water drainage (Trettin et al. 2021). Moreover, WS78 has a significantly (more than 30 times) larger area compared to WS80, which means the lag time of the runoff response will be different between these watersheds.

On the other hand, WS14 is situated at the Coweeta Hydrological Laboratory in North Carolina, characterized by a marine, humid temperate climate and elevations ranging from 675 to 1592 m (Swank and Crossley 1988). The Coweeta Hydrological Laboratory features soils with distinct characteristics. In the northern part of the basin, bedrock consists of granite–gneiss, while the southern part is dominated by mica-schists. Colluvium deposits are found on valley bottoms. The soils fall into two main orders: inceptisols (relatively young soils) and Ultisols (older, more developed soils) with a sandy

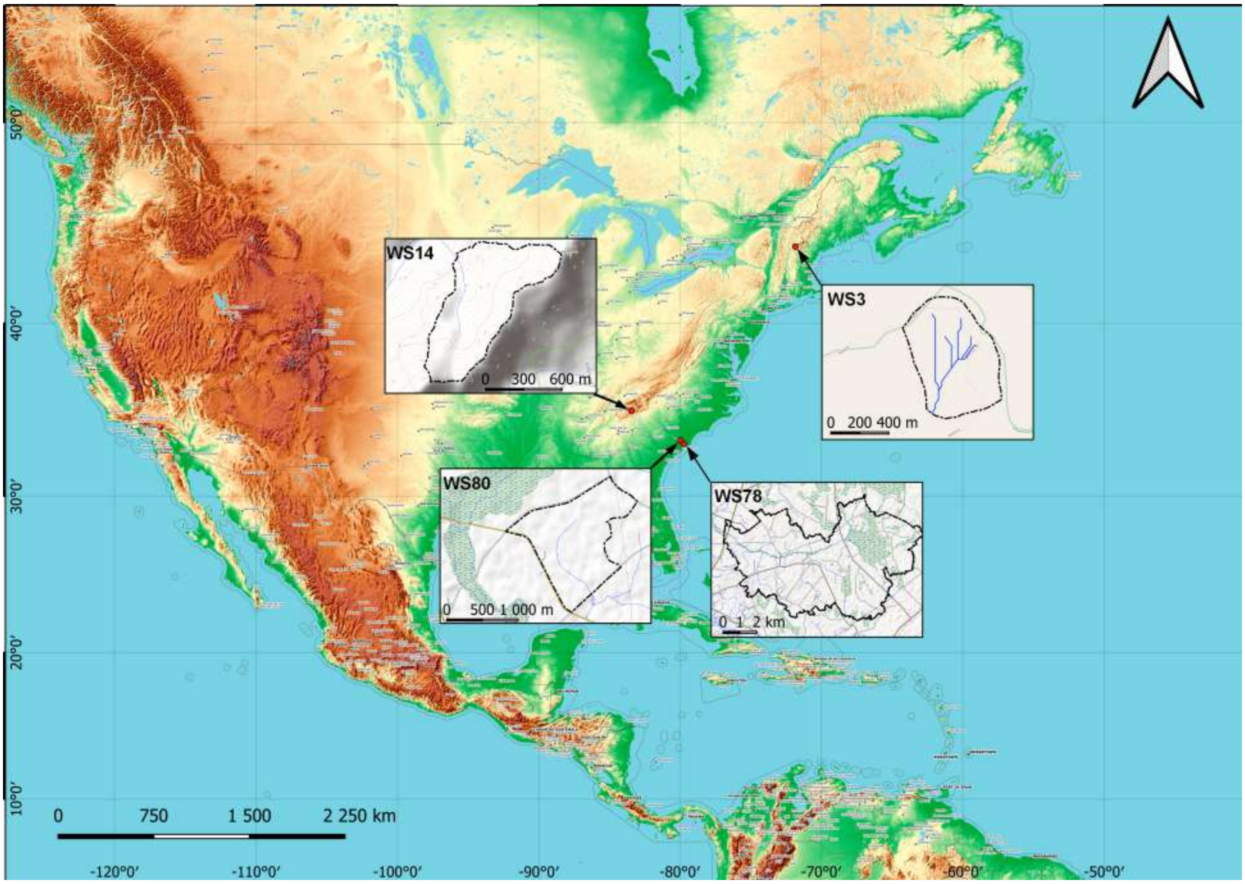

FIG. 1. Location of the investigated catchments.

loam soil category having a colluvial origin and underlain by crystalline igneous and metasedimentary rocks (Miniat et al. 2021).

The Hubbard Brook Experimental Forest, located at the White Mountain National Forest of central New Hampshire, offers a rich ecosystem for research. Its climate features an annual precipitation of approximately 1400 mm, where one-third to one-quarter falls as snow. January averages around −9°C, while July sees an average temperature of 18°C. The forest floor of the site hosts predominantly well-drained Spodosols (Typic Haplorthods) derived from glacial till, characterized by sandy loam textures. These soils are acidic (pH about 4.5 or less) and relatively infertile, with a base saturation of mineral soil at around 10%. The topography varies across the 3138-ha bowl-shaped Hubbard Brook Valley, ranging in elevation from 222 to 1015 m.

Despite the uniform land use (forest cover), the analyzed catchments vary significantly in terms of physiographic characteristics. Maximum catchment areas and slopes are almost 130 times greater than the smallest values for these characteristics. The length of the longest main channel is about 25 times longer than the shortest one. The greatest disparities are observed for the slopes of the main channels, with the slope of WS3 being 635 times greater than that of WS78. The analyzed

TABLE 1. Values of main physiographic factors for the study catchments.

Catchment	Geographical coordinates (centroid)	Area A (km^2)	Length of main channel L (km)	Mean average H_{ave} (MSL)	Mean catchment's slope S (‰)	Average main channel slope I (‰)
WS80	33°9′4.5″N 79°47′33.683″W	1.60	2.00	7.0	4.9	2.1
WS78	33°7′1.513″N 79°43′17.752″W	52.20	19.20	9.0	1.9	0.4
WS14	35°2′59.784″N 83°25′42.383″W	0.60	1.30	902.5	357.6	142.3
WS3	43°57′30.132″N 71°43′14.411″W	0.42	0.72	366.5	282.4	254.2

catchments also differ in their physiographic characteristics (mountainous and lowland watersheds), influencing the development of flood patterns in each of them. The WS80 and WS78 are low-gradient catchments on the coastal plain. The climate is warm humid with a daily average temperature of 17.8°C and average annual rainfall of 1370 mm based on the 1946–2008 period (Dai et al. 2013), with an average of 1470 mm for the recent 9-yr (2011–19) period. Conversely, WS14 is mountainous with an average annual precipitation of about 1840 mm and an average temperature of 12.8°C (Caldwell et al. 2016; Elliott et al. 2017; Laseter et al. 2012). The WS3 catchment is also mountainous, with an average annual precipitation of about 1470 mm and an average temperature of 5.5°C (Green et al. 2021). Hydrologic soil groups C and D identified for WS80 and WS78 indicate soils with high to very high runoff potential. The WS14 and WS3 catchments have dominant soil types with moderate runoff potential (soil hydrologic group B).

3. Materials and methods

The proposed study methodology consists of two main steps. In the first step, a series of peak flows is determined using the EBA4SUB hydrology model. The second step involves calculating design flows based on the generated series from the EBA4SUB model and utilizing the best-fitted statistical distribution. The name of the proposed procedure is design flow calculation using rainfall–runoff model and statistical distribution (DEFRAST). The study was performed using streamflow data from the periods 2004–21 for WS80, 2006–18 for WS78, 1977–2015 for WS14, and 1981–2021 for WS3 catchments. Different study periods were adopted for each catchment due to data availability and specific hydrological conditions. Not all gauging stations were active simultaneously, resulting in varying data availability. Choosing the longest possible observation periods allowed for maximum data utilization and ensured that analyses were based on representative information. Adopting a single study period (2006–15) for all catchments would have resulted in the loss of significant data: 8 years for WS80, 3 years for WS78, 29 years for WS14, and 16 years for WS3. The 2006–15 period would also be too short (only 10 years), and calculating design flows over such a short period could be prone to high uncertainty. The temporal scale for the observed streamflow data was 5–15 min. The data were collected from the U.S. Department of Agriculture Forest Service, Southern Research Station. The study was conducted in the following steps: trend analysis for hydrometeorological data, net precipitation calculation, estimation of peak flow series using the EBA4SUB model, and calculation of design flows using the proposed methodology. The verification of the proposed approach involved comparing the calculated values of the design flows with values from observed time series, as well as values from the GPD method and the Rational Formula.

a. Trend analysis of hydrometeorological data

In the first stage, the trend analysis for hydrometeorological data was performed using the modified Mann–Kendall (MMK) test for a significance level of $\alpha = 0.05$. The S statistics of Mann–Kendall test were estimated with the following formula (Hamed and Rao 1998):

$$S = \sum_{k=1}^{n-1} \sum_{j=k+1}^{n} \mathrm{sgn}(x_j - x_k), \tag{1}$$

$$\mathrm{sgn}(x_j - x_k) = \begin{cases} 1 \ \mathrm{for}(x_j - x_k) > 0 \\ 0 \ \mathrm{for}(x_j - x_k) = 0 \\ -1 \ \mathrm{for}(x_j - x_k) < 0 \end{cases}, \tag{2}$$

where sgn is the signum function and n is the sample size of the time series.

The standard statistics Z was then calculated as

$$Z = \frac{S - \mathrm{sgn}(S)}{\mathrm{Var}(S)^{1/2}}. \tag{3}$$

Variance S [$\mathrm{Var}(S)$] was determined as

$$\mathrm{Var}(S) = \frac{1}{18}[n(n-1)(2n+5)]. \tag{4}$$

The main assumption of the Mann–Kendall test is that autocorrelation does not exist in the time series data. However, in the case of hydrometeorological observations, such correlations may exist and may lead to underestimation of the variance $\mathrm{Var}(S)$. Therefore, an adjustment for variance correction was included, which was calculated only for data with significant partial autocorrelation:

$$\mathrm{Var}^*(S) = \mathrm{Var}(S)\frac{n}{n_s^*}, \tag{5}$$

where n/n_s^* is the correction factor and n_s^* is the effective number of observations.

The correction factor is calculated as

$$\frac{n}{n_s^*} = 1 + \frac{2}{n(n-1)(n-2)} \times \sum_{k=1}^{n-1}(n-k)(n-k-1)(n-k-2)\rho_k, \tag{6}$$

where k is the shift and ρ_k is the value of the next significant autocorrelation coefficient. If the value of Z is lower than the critical value of Z_{crit} ($|1.96|$) for the assumed significance level $\alpha = 0.05$, the trend is considered to be statistically nonsignificant. Otherwise, a trend is statistically significant (may be negative or positive). Trend analysis was conducted for annual daily maximum flows and annual maximum daily precipitation for periods consistent with data availability for the respective catchments: 2004–21 for WS80, 2006–18 for WS78, 1977–2015 for WS14, and 1981–2021 for WS3 catchments.

b. Determination of peak flow series based on the EBA4SUB model

In the next step, peak flow series were determined for the analyzed catchments based on the EBA4SUB model. The calculation was performed based on the following procedure:

estimate of annual maxima rainfall depth for the estimated time of concentration, estimate of average CN parameter for the catchments, designation of net rainfall for rainfall events, and estimates of design hydrograph and peak discharge. Time of concentration T_c was calculated by the Natural Resources Conservation Service (NRCS) method (USDA–NRCS 2010) and the Giandotti formula (Grimaldi et al., 2012b). Since the EBA4SUB model requires a minimum T_c of 1 h, if the calculated T_c was shorter than 1 h, then T_c was assumed to be equal to 1 h. The CN parameter was calculated using the original SCS–CN method (USDA 1986). The net rainfall in the EBA4SUB model is determined using the CN4GA method. The Green–Ampt equation (Green and Ampt 1911) is a physically based infiltration model based on Darcy's law and is expressed as follows:

$$\begin{cases} q_0 = r, \quad \text{for } t < t_p \\ q_0(t) = K_s\left[1 + \dfrac{\Delta\theta\Delta h}{I(t)}\right], \quad \text{for } t \ge t_p \end{cases}, \tag{7}$$

where q_0 is the infiltration rate (mm), t_p is the ponding time (h), Δh is the difference between the depth of water on the soil surface and a constant matric pressure head at the moving wetting front (mm), $\Delta\theta$ is the change in the soil water content (−), and K_s is the saturated hydraulic conductivity (mm h^{-1}).

The value of K_s should not be equated to the laboratory-measured saturated hydraulic conductivity but rather estimated through in situ experiments. It is more practical to refer to an effective value K_{eff} obtained through an optimization procedure. The CN4GA mixed procedure involves the Green–Ampt (GA) infiltration equation in the following steps: (i) estimating total rainfall excess and ponding time using the SCS–CN method and (ii) determining K_{eff} parameter by aligning the GA cumulative infiltration I_{GA} with the corresponding SCS–CN cumulative infiltration $I_{\text{SCS-CN}}$. Average values for GA parameters based on soil type are initially assigned. The estimated I_{GA} is then compared to $I_{\text{SCS-CN}}$. If I_{GA} exceeds (or falls short of) $I_{\text{SCS-CN}}$, the GA is rerun with a lower (higher) K_{eff} value. The K_{eff} parameter is iteratively adjusted until IGA matches $I_{\text{SCS-CN}}$. This iterative process yields an optimal value for effective saturated hydraulic conductivity $K_{\text{eff-opt}}$. Following this, net rainfall is held at zero until the ponding time is reached. Applying GA with the estimated $K_{\text{eff-opt}}$ and known literature values for other GA parameters, the CN4GA rainfall excess amount is computed. The CN4GA net rainfall exhibits the same cumulative rainfall excess and ponding time as the net storm derived by the SCS–CN method (Petroselli et al. 2013).

After determination of the net rainfall, the runoff hydrograph is estimated through the hyetograph convolution of the width function instantaneous unit hydrograph (WFIUH) (Grimaldi et al. 2012a):

$$\text{WFIUH} = \sum_{i=1}^{x} \frac{L_c(i)}{V_c(i)} + \frac{L_h(i)}{V_h(i)}, \tag{8}$$

where L_c, L_h are the channel and hillslope lengths, respectively, for the generic DEM cell i, and V_c, V_h are the channel and hillslope surface runoff velocity, respectively, for DEM cell i.

After defining WFIUH, the runoff hydrograph is defined using the following formula:

$$Q(t) = A\int_0^t \text{WFIUH}(t-\tau)P_n(\tau)d\tau, \tag{9}$$

where A is the catchment area (km^2), t is the rainfall duration (h), and $P_n(\tau)$ is the net rainfall determined by the CN4GA procedure (mm).

The EBA4SUB model is described in detail in Petroselli (2020).

To reduce the percent bias (PBIAS) error of the peak flows $Q_{\max}$ determined using the EBA4SUB model, the linear scaling (LS) approach was applied. The correction technique is described as follows (Yerswa and Chane, 2024):

$$Q_{\max,\text{cor}} = Q_{\max,\text{mod}} \frac{\mu(Q_{\max,\text{obs}})}{\mu Q_{\max,\text{mod}}}, \tag{10}$$

where $Q_{\max,\text{cor}}$—corrected peak flow (m^3 s^{-1}), $Q_{\max,\text{mod}}$—peak flow from the EBA4SUB model (m^3 s^{-1}), $\mu(Q_{\max,\text{obs}})$—the mean value of observed peak flows (m^3 s^{-1}), and $\mu(Q_{\max,\text{mod}})$—the mean value of peak flows from the EBA4SUB model (m^3 s^{-1}).

The corrections to the peak flow values were made for the empirical distribution of these characteristics.

c. *Design flows analysis using statistical distributions*

In the next step, empirical distribution curves were established for both the observed peak flows and for those obtained from the EBA4SUB model. To accomplish this, peak flow values were ranked in a cumulative distribution from highest to lowest. Next, empirical probabilities and return periods were determined using the ranking formula method:

$$p = \frac{m}{N+1}, \tag{11}$$

where m is the rank of peak flow for the cumulative distribution and N is the number of observations.

Empirical probability p is related to the return period (RP) by the following relationship:

$$\text{RP} = \frac{1}{p}(\text{years}). \tag{12}$$

After that, design flows Q_T were determined using Pearson's type III (PIII), Weibull's (W), and lognormal (L-N) statistical distributions based on the following formulas (Młyński et al. 2019):

The PIII distribution:

$$Q_T = \varepsilon + \frac{t(\lambda)}{\alpha}. \tag{13}$$

Weibull (W) distribution:

$$Q_T = \varepsilon + \frac{1}{\alpha}[-\ln(1-p)]^{1/\beta}. \tag{14}$$

TABLE 2. Pond and swamp adjustment factor F_p (USDA 1986).

Percentage of pond and swamp areas	F_p
0	1.0
0.2	0.97
1.0	0.87
3.0	0.75
5.0	0.72

TABLE 3. PBIAS statistics ranges and associated performance ratings.

Performance rating	PBIAS (%)
Very good	$-10 < \mathrm{PB} < +10$
Good	$\pm10 \le \mathrm{PB} < \pm15$
Satisfactory	$\pm15 \le \mathrm{PB} < \pm25$
Unsatisfactory	$\mathrm{PB} \ge \pm25$

Lognormal (L-N) distribution:

$$Q_T = \varepsilon + \exp(\mu + \sigma u_p), \tag{15}$$

where ε is the lower limit of the series; λ, β are the shape parameters; α is the scale parameter; μ, σ are the parameters of the lognormal distribution; p is the probability of exceedance; and u_p is the quantile of p order.

The values of the distribution parameters were estimated by using the maximum likelihood estimation method. The Kolmogorov–Smirnov test was adopted to test the consistency of the theoretical distribution with the empirical distribution (Radevski et al. 2016). The best-fitted distribution was selected based on the rank of the peak-weighted root-mean-square error (PWRMSE). The PWRMSE method was described by Wałęga (2016). The calculations of design flows, using statistical distributions, were conducted for both the observed time series and peak flow series generated by the EBA4SUB model.

d. Design flows analysis using empirical formulas

In the next stage, design flows were estimated using two empirical methods, i.e., the GPD method and RF. The GPD method is an official method currently used by USDA (1986), and it can be described as follows:

$$Q_T = q_u A Q F_p, \tag{16}$$

where Q_T is the design flow for an assumed probability of exceedance (m^3 s^{-1}), q_u is the unit peak discharge [(m^3 s^{-1}) (cm km^2)$^{\phi 1}$], A is the drainage area (km^2), Q is the runoff from a 24-h storm with a given return period T (cm), and F_p is the pond and swamp adjustment factor.

Runoff Q was estimated from the original SCS–CN method (USDA 1986). The CN parameter was calculated as a weighted average value for different forest types and hydrological soils groups assuming the average level of antecedent soil moisture [antecedent moisture condition (AMC-II)]. The pond and swamp adjustment factor was established based on Table 2.

If the percentage of pond and swamp areas exceeds 5%, then consideration should be given to routing the runoff through these areas.

The unit peak discharge q_u can be obtained from the empirical formula:

$$\log(q_u) = C_0 + C_1 \log t_c + C_2(\log t_c)^2 - 2.366, \tag{17}$$

where C_0, C_1, C_2 are the coefficients of functions of Ia/P for a particular rainfall type (−); Ia is the initial abstraction (mm); P is the 24-h rainfall with the assumed return period that causes the runoff Q (mm); and T_c is the time of concentration (h).

The RF (Kuichling 1889) is the most common approach for estimating the design peak discharge for small catchments and is given as

$$Q_T = 0.0028\, C \frac{h_c}{T_c} A, \tag{18}$$

where Q_T is the design flow for an assumed probability of exceedance (m^3 s^{-1}), C is the runoff coefficient (−), h_c is the critical rainfall depth for an assumed return period (mm), T_c is the time of concentration (h), and A is the catchment area (ha).

d. Evaluation of methods to calculate design flows

In the last stage of the study, the results of calculated design flows by the proposed approach (DEFRAST) were verified. The verification involved comparing the calculated design flows with those from the observations and calculating the PBIAS values. Additionally, PBIAS values were determined for both the GPD and Rational Formula to identify the best method for calculating design flows in ungauged catchments. The PBIAS is described as (Ajmal et al. 2020)

$$\mathrm{PBIAS} = \frac{\sum_{i=1}^{n}(Q_T - Q_{T,m})}{\sum_{i=1}^{n} Q_T} \times 100(\%), \tag{19}$$

where Q_T is the discharge related to a return period, calculated using the statistical distribution for the observed time series (m^3 s^{-1}), and $Q_{T,m}$ is the discharge related to a return period, estimated using the GPD, RF, and DEFRAST approaches (m^3 s^{-1}).

A negative value of PBIAS indicates an overestimation, while a positive value indicates underestimation of the observed values. A qualitative evaluation of the PBIAS index values is given in Table 3.

4. Results and discussion

a. Trend analysis for hydrometeorological data

Trends of the annual maxima of hydrometeorological data (precipitation P and streamflow Q) in each catchment are investigated using the MMK method. The results of the MMK test are presented in Fig. 2 and Table 4.

The results presented in Fig. 2 indicate that the periods of peak flows and annual daily maximum precipitation do not

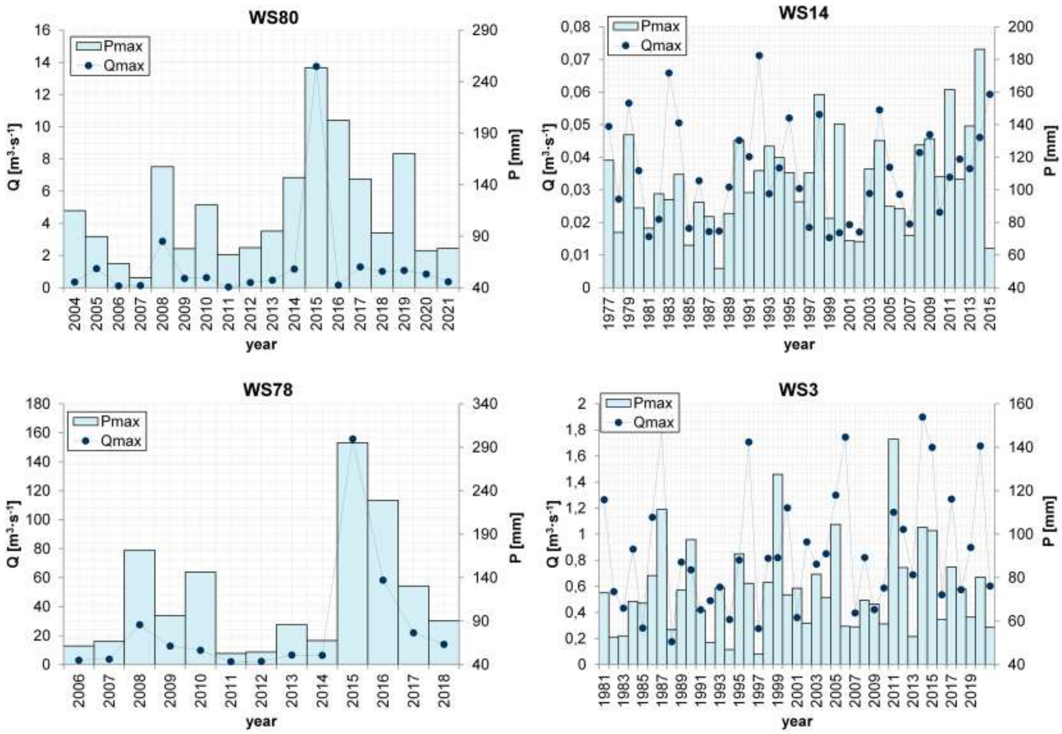

FIG. 2. Annual maxima time series for peak flow rates Q and daily precipitation P in the study catchments.

coincide. This occurs because catchments, especially forested ones, do not respond linearly to rainfall, and the lag time between rainfall and runoff varies. Based on the findings presented in Table 4, it was determined that the Z statistics were lower than the critical value of 1.96, suggesting statistically insignificant trends at the 0.05 significance level for the analyzed time series for all catchments. This means that no factors affecting the formation and trend of annual maximum flows and precipitation occurred during the study period at these catchments, although a more reliable trend analysis requires the analysis of data from neighboring catchments as well. Despite observed climate changes on a large scale in the region, their relationship with hydrometeorological factors in these small-scale forested catchments is inherently nonlinear. Overall, the results are consistent with recent studies (Folton et al. 2019; Anderegg 2020), stating that forests have considerable potential to help mitigate potential climate changes. This makes the quantification of potential changes in water resources including storm event characteristics, due to the influence of climate change, challenging. However, these results are critical for understanding the complex functioning of hydrological systems and for developing effective water management strategies in response to evolving climate conditions.

TABLE 4. Results of trend analyses for the study catchments.

	Z statistic	
Catchment	Peak flow	Precipitation
WS80	0.833	0.985
WS78	1.281	1.037
WS14	0.545	1.770
WS3	1.416	0.840

b. *Net rainfall analysis*

The proposed DEFRAST methodology for determining design flow values requires the establishment of an observational series of annual maximum rainfall with a duration equal to the time of concentration T_c. For each such episode, the net rainfall was determined using the SCS–CN method. The results of the calculations are summarized in Fig. 3.

The T_c values were calculated as 2.06 and 21.76 h for the WS80 and WS78 catchments, respectively. This large variation in T_c was primarily due to the catchment physiographic characteristics (e.g., drainage area, stream channel length, etc.). For example, T_c values for WS14 and WS4 were the lowest due to their small sizes (drainage area of less than 1 km^2). In the case of the WS80 catchment, T_c was estimated using the NRCS method (USDA–NRCS 2010). This value was defined in the study conducted by Wałęga et al. (2020) . For the WS78 catchment, T_c was estimated using the Giandotti method (Grimaldi et al., 2012b). In the case of the WS14 and WS4 catchments, T_c was also determined by the NRCS method. These values were approximately 20 min (Wałęga et al. 2020), but a value of 1 h for these catchments was used as the minimum value required by the EBA4SUB model. In the analysis, varied methods for determining the time of concentration were assumed because the study catchments are characterized by differences in hydrographic, physiographic, and geomorphological

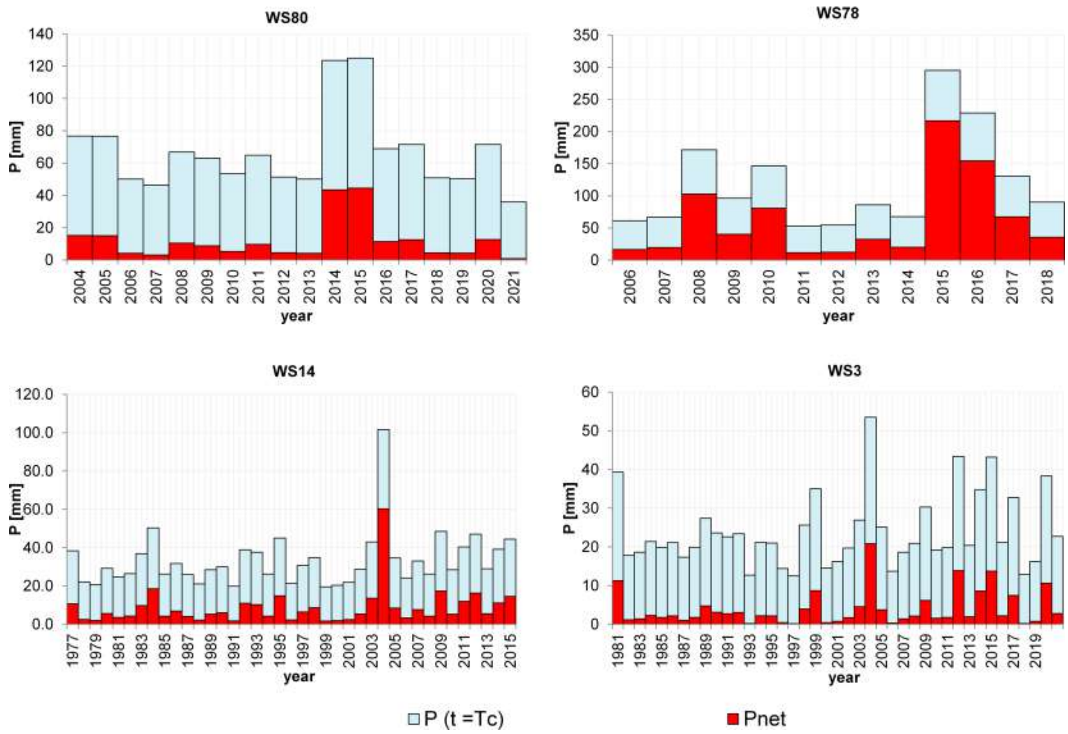

FIG. 3. Total rainfall (P for T_c) and calculated net rainfall P_{net} for the study catchments.

features and diverse meteorological conditions. Each of these factors affects the way water moves within the catchment, necessitating a specific approach to calculations. Therefore, methods for calculating the time of concentration were selected based on the characteristics of the catchments. The minimum, average, and maximum total precipitation for the WS80 were obtained as 36, 67, and 125 mm, respectively. On the other hand, the minimum, average, and maximum total precipitation for the WS78 were recorded as 53, 119, and 295 mm, respectively. The minimum was 20 mm, the average was 33 mm, and the highest was 102 mm for the WS14 catchment. Similarly, the minimum, average, and maximum precipitation for the WS3 were 13, 24, and 54 mm, respectively.

The net rainfall P_{net} for the individual catchments was calculated assuming levels of moisture that ensure the formation of direct runoff. This approach is necessary because the obtained net rainfall values are used to determine a series of peak flows Q_{max} using the EBA4SUB model and later design flows using statistical methods. Zero values lead to the absence of peak flows in the given series, which is inconsistent with observations, as Q_{max} has been recorded in each catchment in individual years. Zero values of P_{net} translate into zero Q_{max} values, which makes it impossible to further calculate design flows using statistical methods based on the series generated by the EBA4SUB model. For the WS80 and WS78 catchments, calculations were performed for AMC(II), while for the WS14 and WS3 catchments, calculations were performed for AMC(III). Based on Fig. 3, it was found that in the WS80 catchment, P_{net} values ranged from 0.9 to 44.5 mm, with an average of 11.9 mm. In the case of the WS78 catchment, P_{net} ranged from 11.5 to 216.7 mm, with an average of 62.4 mm. The WS14 catchment was characterized by P_{net} values ranging from 1.7 to 60.2 mm, with an average of 8.6 mm. The WS3 catchment had the lowest P_{net} values among the analyzed catchments, ranging from 0.2 to 20.8 mm, with an average of 3.9 mm.

The SCS–CN method is one of the most widely used approaches for determining net rainfall. However, it has several limitations due to its empirical origins. Developed primarily from regional data for agricultural sites where it performs well, the SCS–CN method may not be directly applicable to other types of regions without adjustment. Additionally, the method does not account for spatial variability in runoff, as it assumes homogeneous conditions for the runoff process (Bartlett et al. 2016). Another significant limitation of the SCS–CN method is defining the appropriate AMC level, which is traditionally determined based on the 5-day antecedent rainfall depth. However, soil moisture measurements within the area of interest may provide a more accurate basis for selecting the AMC level. Improved understanding of the relationship between antecedent soil moisture and CN values could significantly enhance runoff estimation (Shi and Wang 2020). Meteorological data are also critical in determining AMC, as they provide insights into how atmospheric conditions influence soil moisture (Ali and Roy 2010). Historical time series of meteorological data can reveal patterns in rainfall timing and intensity that impact soil moisture dynamics (Wasko et al. 2020). Additionally, local soil characteristics, such as texture and physical properties, play a crucial role in water retention and should be considered when determining

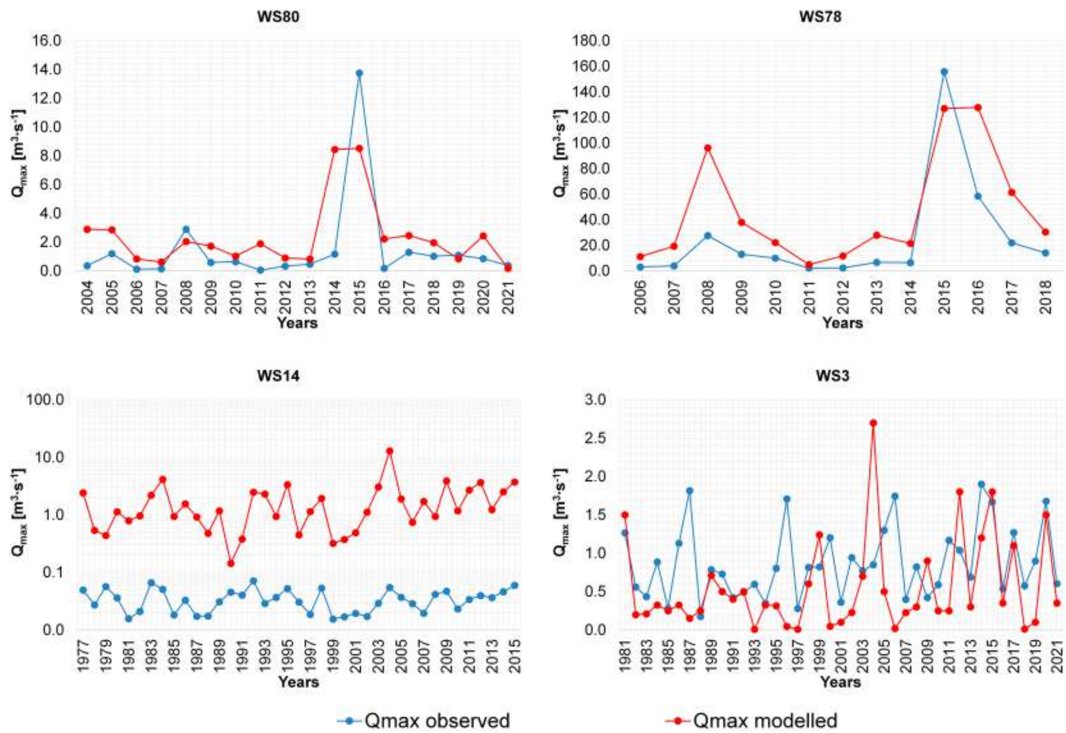

FIG. 4. Results of peak discharge calculated by the EBA4SUB model for the study catchments.

AMC levels (Li et al. 2022). Verification of AMC levels through actual measurements and observations is essential for ensuring accuracy. This process not only improves result quality but can also inform the development of new techniques for AMC determination. For example, Hettiarachchi et al. (2019) proposed a modified SCS–CN approach that incorporates observed soil moisture to better identify AMC levels. Given the temporal and spatial variability of soil moisture, regular updates and trend analyses of relevant data are necessary to adapt AMC levels to changing environmental conditions (Huang et al. 2016).

c. *Peak discharge modeling using EBA4SUB*

In the next stage of the analysis, based on the observed maximum rainfall series for a duration equal to the time of concentration and the specified net rainfall amounts, peak flow series Q_{max} were determined using the EBA4SUB model. The results are presented in Fig. 4.

Plots in Fig. 4 indicate that, in general, the EBA4SUB model overpredicted the peak discharge rates. For the WS80 catchment, the smallest discrepancy between the observed and calculated Q_{max} was found for the year 2019, where the difference between peak flows was 25%. The largest disparity occurred in 2011, a relatively dry year, when the peak flow from the EBA4SUB model was 35 times greater than the observed value. The results for the WS78 catchment showed that the smallest difference between the observed and calculated Q_{max} occurred in 2015 with an extreme flow in October, with a difference of 20%. The largest discrepancy was noted for the year 2012 also a relatively dry year, when the peak flow from the EBA4SUB model was 5 times greater than the observed flow rates. For the WS14 catchment, it was found that the EBA4SUB model substantially overestimated peak discharges, as compared to observed maxima. The observed peak flows in WS14 are the lowest among all analyzed catchments. Hence, even the low differences between the calculated and observed rates yielded a high percentage of disproportion. In addition, these differences may have been caused by the time of concentration assumed to be as 1 h, a minimum required by the model, despite the subhourly value found for WS14 with an area of only 0.6 km^2. Based on the results presented in Fig. 4, it can be observed that the peak flows for WS14, simulated using the EBA4SUB model, are significantly higher than the observed values, despite the assumed time of concentration being 1 h, which is longer than the actual time of around 20 min. The proposed methodology requires the creation of annual maximum precipitation series with durations close to the time of concentration. In the case of catchment WS14, the precipitation depths for the assumed time of concentration of 1 h are significantly higher than for the actual time of around 20 min. Consequently, the simulated peak flows using the EBA4SUB model are inflated. For catchment WS3, there is an observed underestimation of peak flows using the EBA4SUB model, which results from the discrepancy between the assumed time of concentration (longer than the actual time) and precipitation episodes with durations equal to 1 h compared to episodes with durations close to the actual time of concentration. Assuming a longer time of concentration for small catchments, which actually have a shorter time of concentration, can potentially lead to consequences in

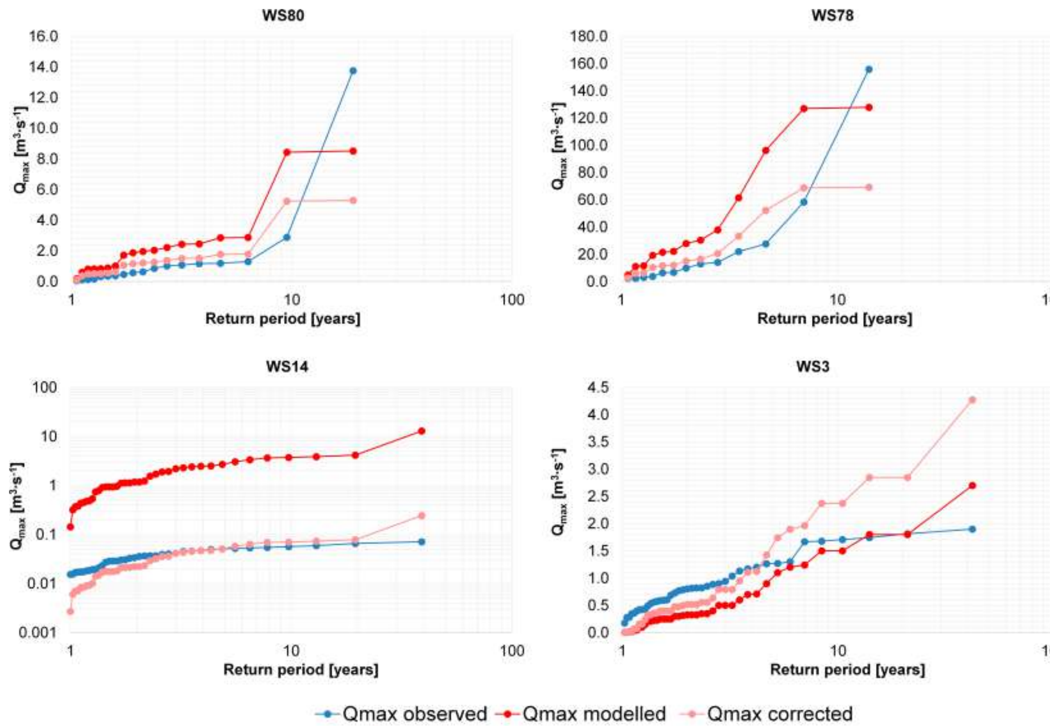

FIG. 5. Empirical flood frequency curves for observed and the EBA4SUB model–generated peak discharges for the study catchments.

forecasting and modeling peak flows. This primarily affects two main aspects: underestimation of peak flows and delay in the peak flow timing. Underestimation of peak flows and time to peak arise from the incorrect assumption about the rate at which water reaches the catchment outlet after precipitation event. In small catchments, which have a shorter time of concentration, water reaches the main streams of the catchment more quickly, resulting in rapid and high peak flows. However, if the hydrological model assumes a longer time of concentration, it predicts that water will flow more slowly, which leads to underestimated peak flows and a longer runoff hydrograph (the same volume of water from net precipitation must be distributed over a longer time in the unit hydrograph). The delay in peak flow timing is another effect of assuming an extended time of concentration. Models that assume a longer time of concentration predict that peak flows will occur later than they actually do under real conditions. In small catchments with a shorter time of concentration, peak flows occur sooner after precipitation. This circumstance tends to suggest that the EBA4SUB model should be used for catchments where T_c is $\geq$1 h. For the WS3 catchment, the EBA4SUB model was tested only for the AMC-III which results in direct runoff. The results indicate that only in 6 out of the 41 events, the EBA4SUB model overestimates peak flow rates. Although the area of WS3 is smaller than WS14 (0.424 km^2), the observed peak flows on it are greater than the latter. This is because of substantial soil moisture the WS3 catchment receives in the form of snowmelt and precipitation even if there is a limited amount of rainfall during the storm episode. A study conducted by Mateo-Lázaro et al. (2019) and Barnett et al. (2005) indicated that snowmelt can comprise 50% or more of the total runoff (net rainfall and snowmelt), suggesting a higher value of CN parameter for snowmelt–rainfall–runoff conditions as compared to simple rainfall–runoff events (Hejduk et al. 2015).

In the next step, the empirical flood frequency curves for maximum flows from observations were compared with those calculated by the EBA4SUB model ($Q_{\max}$ modeled) and the bias-corrected values from EBA4SUB using the linear scaling technique ($Q_{\max}$ corrected) (Fig. 5). Results showed that, in most cases, the EBA4SUB model produces higher flow values within the context of flood frequency curves. This trend is particularly evident for longer return periods. To improve the model results, linear scaling correction was applied, which in the vast majority of cases allowed for better alignment of the calculated values with observations, especially for shorter return periods. A detailed analysis of the results indicates that, in the WS80 and WS78 catchments, the overestimation of results is particularly noticeable for longer return periods, with the exception of the longest return periods, which were 19 and 14 years for WS80 and WS78, respectively. The linear scaling correction effectively reduces discrepancies, bringing the values from EBA4SUB closer to the observed values. In the case of the WS14 catchment, the EBA4SUB model exhibits the largest discrepancies. The flows obtained from the model are very high compared to the observed values. However, the applied correction significantly reduces these values, making them much closer to the actual ones. The best results are observed

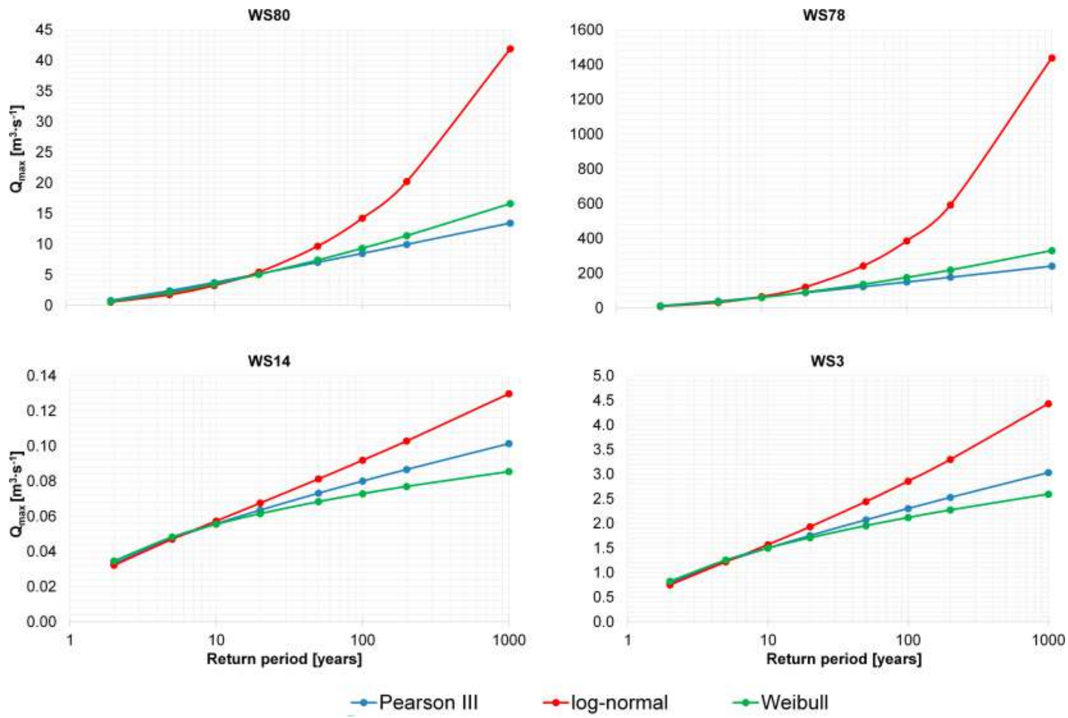

FIG. 6. Results of design flow analysis by statistical distribution for the study catchments.

when comparing the flood frequency curves for WS3, where the EBA4SUB model demonstrates the highest quality of performance. It should be emphasized that the applied correction inflates flow values in the longer return period range. For shorter return periods, the corrected values are close to the observations. This phenomenon is due to the high ratio of average observed peak flows to peak flows from EBA4SUB, which was nearly 1.6. Since for the series prior to correction, the peak flow values from EBA4SUB for longer return periods were close to the observed values, the introduction of the correction increased the discrepancies for these return periods.

d. *Design flows analysis*

In the next stage, the results of design flows analyzed using statistical distributions, with the best fit identified based on the PWRMSE rank, are presented in Fig. 6 and Table 5.

Based on the results presented in Fig. 6, it can be concluded that the highest values of design flow were for the lognormal (L-N) distribution. The lognormal distribution is heavy tailed, which is why it has a tendency to yield higher values of quantiles for a low probability of exceedance as compared to the Weibull (W) and PIII distributions. The heavy-tailed distributions of flood frequency are characteristics to the drier regions, where flooding tends to be generated by heavy rainfall and infiltration excess overland flow (Merz et al. 2022). In the humid regions, shallow subsurface outflow and saturation excess overland flow dominate the flood generation mechanism (Wałęga and Amatya 2020; Amatya et al. 2022). In a study conducted in forested catchments of coastal South Carolina, subsurface outflow was suggested contributing to a major portion of the total runoff. As such, nonheavy-tailed distributions can be more suitable for flood frequency analysis. Based on Table 5, it can be concluded that PIII is one of the best-fitted distributions in this case which is consistent with (Amatya and Radecki-Pawlik 2007) who used the same distribution for the analysis of flow dynamics in forested catchments in coastal South Carolina.

TABLE 5. Rank of best-fitted statistical distribution based on the PWRMSE for the study catchments.

Catchment	L-N	PIII	W
WS80	1	3	1
WS78	1	2	3
WS14	3	1	2
WS3	3	1	1
Σ	8	7	7

In the next step, design flow values calculated using the GPD method (GPDM), RF, and the new proposed approach DEFRAST were compared against the values from the best-fitted statistical distribution, which is Pearson type III. Due to the large area of the WS78 catchment exceeding the recommended size, the Rational Formula was not applied. Figure 7 presents the flood frequency curves for the analyzed methods.

Results presented in Fig. 7 showed that, in most cases, the DEFRAST method provides design flow results that are close to, albeit slightly overestimated, the baseline values determined using the Pearson type III distribution. These results are particularly evident for longer return periods, such as 1000 and 200 years. The corrected version of the DEFRAST

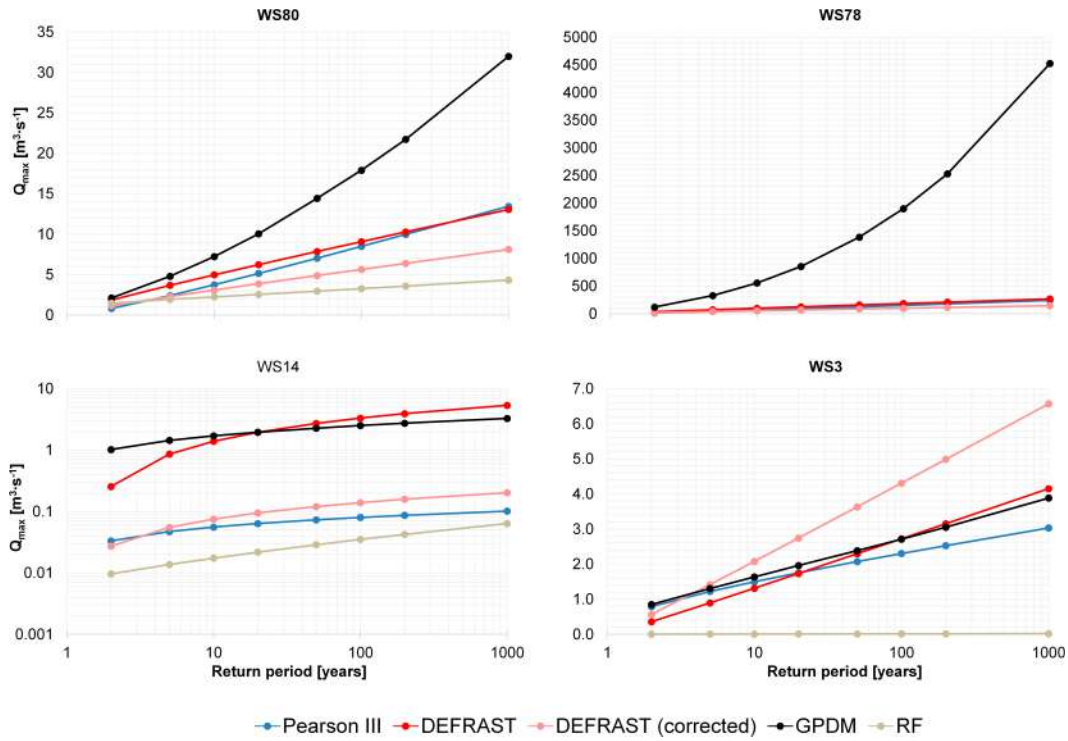

FIG. 7. Design flows calculated by empirical formulas for the study catchments.

method (DEFRAST-corrected), through linear scaling, yields lower design flow values than the uncorrected version, bringing them even closer to the results from the Pearson type III distribution. The greatest discrepancies between the results from the DEFRAST method and the Pearson type III distribution were observed for the WS14 catchment. However, applying the linear scaling correction significantly reduced these discrepancies. The GPD method shows a significant overestimation of design flows compared to the Pearson type III distribution, especially for large return periods (1000 yr). This is most evident in the WS78 catchment, where design flow values calculated using the GPDM are even several dozen times higher than the baseline values obtained from the Pearson type III distribution. Similar results were obtained by Wałęga et al. (2020) who also pointed out significant discrepancies in the values of design flows obtained using the GPD method for catchments with similar characteristics. Generally, the results from the GPD method are less consistent with the Pearson type III distribution, particularly in large catchments (like the WS78) and for long return periods, which may suggest limitations of this approach in accurately representing actual peak discharges under specific conditions. The smallest differences between the values from the GPD method and the Pearson type III distribution were found for the WS3 catchment. The RF method yielded underestimation of design flows compared to the results obtained from the Pearson type III distribution, regardless of the studied catchment and return period. The best results for the RF were found for the WS14 catchment, where the design flow values from this method were similar to those from PIII distribution. Generally, the RF performs well in small forested catchments because it accounts for a simple relationship between rainfall and runoff, which corresponds to their short concentration times and uniform conditions, such as vegetation cover and retention. This is confirmed by studies by Amatya et al. (2021b) as well as Mukherjee et al. (2024), which showed that the RF can provide good estimates of design flows under suitable conditions, but its effectiveness depends on the size and characteristics of the catchment, highlighting the need for careful calibration. At the same time, it should be emphasized that in the other catchments, values calculated using the RF are generally significantly lower than those from the statistical method, indicating the limited usefulness of this method for estimating design flows.

In the GPD method, one of the crucial parameters is the pond and swamp adjustment factor F_p. If the area of the pond and swamp in the catchment of interest is 5% or larger, then F_p assumes a default value of 0.72 (USDA–NRCS 2010). A study conducted by Wałęga et al. (2020) indicated that this value should not be used for forested catchments because of the high retention capacities of forested catchments. According to the authors, the F_p value should be lower than 0.40 for the forested catchments they studied. Also, they revealed significant relationships between F_p values and rainfall depth as well as duration. On the other hand, the Rational Formula exhibits some limitations, including the one associated with the estimation of the runoff coefficient, C. First, the C values were not developed through the calibration in experimental catchments as was recently done by Amatya et al. (2021b)

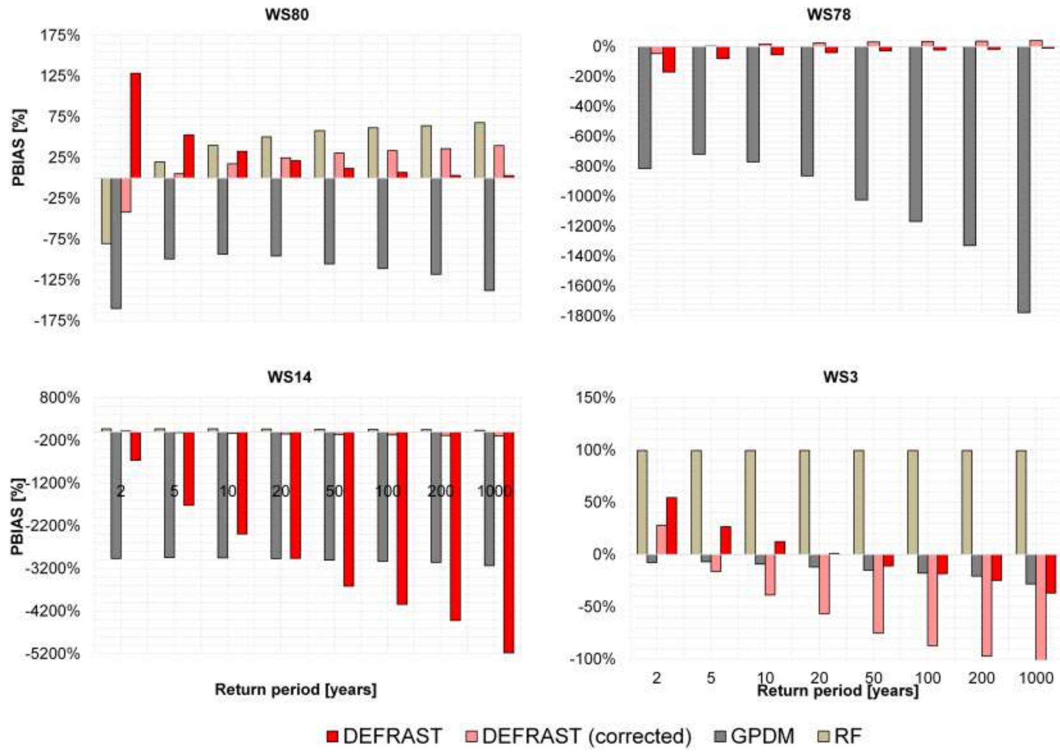

FIG. 8. PBIAS values calculated for three analyzed methods (GPD, RF, and DEFRAST).

and Mukherjee et al. (2024), but by consultations with experts. The selection of appropriate C values including from literature can be subjective with some uncertainties and can impact the estimation of the peak discharge. The second limitation is the assumption of the critical duration of rainfall, which can lead to the underestimation of peak discharges (Grimaldi and Petroselli 2015).

A major limitation of both GPD and RF is the need for a design rainfall depth for estimating peak discharges with a given probability of exceedance. Hence, a statistical distribution describing rainfall depth must be selected. It should be emphasized that both GPD and RF are empirical equations which were based on hydrometeorological data collected during the last century. Taking into account the changes in land use and climatic patterns observed in recent decades and limited availability of current multisite measurement data, the wide use of existing empirical formulas using the above parameters may be questionable. Therefore, it is important to come up with a novel methodology to calculate design flows for ungauged catchments, which should be helpful for understanding mechanisms of peak flow generation (Liu et al. 2017). The proposed approach to calculating design flows in DEFRAST is based on rainfall–runoff modeling using the EBA4SUB model. In general, the EBA4SUB model has shown promising results in predicting design flows. For example, Recanatesi and Petroselli (2020) applied the model to calculate design flows for flood mapping in Italy. They have concluded that the results from the EBA4SUB model can serve as the basis for assessing the increased flood risk. Petroselli et al. (2019a) evaluated the model for design flow calculations in selected catchments in Iran. They pointed out that the EBA4SUB model has the potential to serve as a viable tool for predicting design peak flows in Iran. This recommendation gains even more significance when the model is combined with a hydraulic framework to facilitate the updating of flood hazard maps. Houessou-Dossou et al. (2022) tested the model for flood frequency calculations in the catchments Kakia and Esamburumbur located in Kenya, Africa. Their study highlighted the significance of the EBA4SUB model in estimating design hydrographs in ungauged catchments, simultaneously revealing the correlation between rainfall frequency analysis and flood frequency analysis in small catchments. In addition, Młyński et al. (2020) proposed a new approach of flood frequency estimation based on the EBA4SUB model. They pointed out that the proposed methodology is characterized by a low relative error for design flows, making it advantageous to apply the EBA4SUB model. However, it should be emphasized that the EBA4SUB model so far has not yet been tested in small forested catchments.

e. Verification of methods to calculate design flows

Finally, the performance assessment of the various methods for determining design flow magnitudes for ungauged catchments was conducted using the percent error indicator, PBIAS. The magnitude of the indicator was determined by comparing the design flow values between the methods for ungauged catchments and the Pearson type III distribution for observed data. The results are presented in Fig. 8.

TABLE 6. PBIAS performance rating for the analyzed methods of calculating design flows.

Method	RP 100	50	20	10
		WS80		
DEFRAST	Very good	Good	Satisfactory	Unsatisfactory
DEFRAST-corrected	Unsatisfactory	Unsatisfactory	Satisfactory	Satisfactory
GPD	Unsatisfactory	Unsatisfactory	Unsatisfactory	Unsatisfactory
RF	Unsatisfactory	Unsatisfactory	Unsatisfactory	Unsatisfactory
		WS78		
DEFRAST	Satisfactory	Unsatisfactory	Unsatisfactory	Unsatisfactory
DEFRAST-corrected	Unsatisfactory	Unsatisfactory	Satisfactory	Satisfactory
GPD	Unsatisfactory	Unsatisfactory	Unsatisfactory	Unsatisfactory
RF	—	—	—	—
		WS14		
DEFRAST	Unsatisfactory	Unsatisfactory	Unsatisfactory	Unsatisfactory
DEFRAST-corrected	Unsatisfactory	Unsatisfactory	Unsatisfactory	Unsatisfactory
GPD	Unsatisfactory	Unsatisfactory	Unsatisfactory	Unsatisfactory
RF	Unsatisfactory	Unsatisfactory	Unsatisfactory	Unsatisfactory
		WS3		
DEFRAST	Satisfactory	Good	Very good	Good
DEFRAST-corrected	Unsatisfactory	Unsatisfactory	Unsatisfactory	Unsatisfactory
GPD	Satisfactory	Satisfactory	Good	Very good
RF	Unsatisfactory	Unsatisfactory	Unsatisfactory	Unsatisfactory
PBIAS range	Very good	Good	Satisfactory	Unsatisfactory

Based on the results presented in Fig. 8, it was found that for the WS80 catchment, the DEFRAST method yielded low estimation errors for design flows, especially for high recurrence intervals. The PBIAS values ranged from −12% to 3% for recurrence intervals from 50 to 1000 years, respectively. As the recurrence interval decreases, the PBIAS values increase. For DEFRAST-corrected, the recomputed errors also remain at a relatively low level; however, they are greater than those for the DEFRAST. In general, DEFRAST-corrected provided mostly positive PBIAS. In the case of DEFRAST, for recurrence intervals from 2 to 200 years, PBIAS is negative, indicating higher design flow values from this model compared to the Pearson type III distribution. The GPD method yielded the highest negative PBIAS values, ranging from −93% to −160% overestimate of design flows. However, in the case of the Rational Formula, positive PBIAS values were obtained for all recurrence intervals except for 2 years, with values ranging from 20% to 68%, indicating underestimates. For the 2-yr return period, the PBIAS was −80%. For WS78 catchment, the highest PBIAS values were obtained for the GPD method, with design flow values even 14 times higher than those for the Pearson type III distribution (negative values of PBIAS). The DEFRAST method provided design flow values that were much closer to those from the Pearson type III distribution, with very low PBIAS for high recurrence intervals. Similar to WS80, as the recurrence interval decreased, the PBIAS values increased. The DEFRAST-corrected approach yielded a higher PBIAS than DEFRAST for high recurrence intervals, but as the intervals decreased, the PBIAS values also decreased. For the WS14 catchment, the highest PBIAS values were identified for DEFRAST and GPDM (negative values), while relatively low PBIAS was determined for the Rational Formula, with positive values ranging from 37% to 71%, indicating an underestimation of design flows compared to the Pearson type III distribution. DEFRAST-corrected yielded significantly better results than DEFRAST, with the average absolute PBIAS error for DEFRAST-corrected being lower than that for the Rational Formula. For the WS3 catchment, the DEFRAST and GPD methods were identified as the best methods based on the PBIAS performance statistics. In the case of the Rational Formula, the PBIAS error remained constant at 100% for each recurrence interval. In summary, the DEFRAST and DEFRAST-corrected methods exhibit the best performance in predicting design flows, which was particularly evident in the WS80, WS78, and WS3 catchments. In the WS14 catchment, DEFRAST significantly exceeds the results from Pearson type III distribution, although its correction resulted in a substantial reduction in differences. The GPD method is the least stable, with very high overestimation in the WS78 and WS14 catchments. The Rational Formula consistently yields underestimated results in all catchments, making it less adequate for analyzing design flows, especially for longer return periods. The results clearly indicate that the proposed DEFRAST approach could serve as an alternative for calculating design flows. Since the results may require adjustment, it is necessary to specify the thresholds (catchment area, recurrence intervals) at which such corrections should be made. The performance evaluation of the methods is provided below as a summary of the PBIAS performance rating for the calculated design flow values. Since, from the perspective of designing technical infrastructure in small catchments, the most important design flows are Q100–Q10, Table 6 summarizes the PBIAS performance rating for such design flows.

Table 6 confirms that the DEFRAST method provides the best quality results, especially for larger return periods, such as Q100 and Q50. The GPD and RF methods mostly achieved unsatisfactory quality, regardless of the analyzed return period and catchment area. The obtained results confirm that the DEFRAST method and its correction could serve as an alternative for calculating design flows, mainly in the Q100–Q10 range. This is particularly important because these flows are widely used in the design of technical infrastructure, such as drainage systems, dams, channels, and other hydraulic engineering structures. Quantiles Q10 and Q20 are particularly relevant for projects with medium-risk levels, while Q50 and Q100 are crucial for high-risk or critical projects (Ali and Rahman 2022).

5. Conclusions

The main objective of this study was to explore a new approach (DEFRAST) to calculate design flows in ungauged forested catchments and compare its performance relative to two widely used methods in ungauged catchments such as the Graphical Peak Discharge (GPD) method and the Rational Formula (RF). The proposed DEFRAST approach consists of two main steps: the first step involves the peak flow series modeling using the EBA4SUB model followed by the second step involving calculation of design flows based on the EBA4-SUB-generated series and the best-fitted statistical distribution based on observed annual peak flow data. The study was conducted in the following steps: trend analysis for hydrometeorological data, net rainfall calculation, estimation of peak flow series using the EBA4SUB model, and calculation of design flows using the proposed DEFRAST methodology. To reduce the PBIAS error in design flows obtained using DEFRAST, the linear scaling technique was applied. The results of the analysis suggest that

1) The modified Mann–Kendall test revealed no significant trends in the hydrometeorological time series (P and Q) for the study catchments, indicating the constancy of factors determining the stationarity of the hydrometeorological data.
2) Pearson type III distribution was found to be the best-fitted statistical distribution, among the three analyzed: Pearson type III distribution, lognormal, and Weibull, for modeling design flow in the investigated catchments. The form of the statistical distribution may result from the characteristics of the catchments mitigating intense rainfall.
3) Among the two empirical formulas evaluated to calculate the flood frequency, the GPD method highly overestimated design flows, while the RF led to underestimation of design discharges. Thus, the results obtained in this study clearly indicate a need to further verify the empirical formulas tested in this study, including their parameters like runoff coefficient, F_p factor, and time of concentration on catchments in varying ecohydrological regions for increasing confidence in their wider applications.
4) Based on the obtained PBIAS values as a performance indicator, it can be stated that the DEFRAST or DEFRAST-corrected approaches exhibited the lowest values. This indicates that the proposed methodology can be an alternative to empirical formulas for determining project flow magnitudes in ungauged catchments. Due to its complexity, the proposed DEFRAST methodology, which combines hydrological modeling and statistical analyses simultaneously, can also be applied in catchments with characteristics different from those presented in this study.

It is also equally important to highlight the limitations of determining design flows using the proposed DEFRAST approach. The main limitations include the simplification of complex hydrological processes; the quality of input data; calibration in ungauged catchments; lack of consideration for ongoing climate changes; a focus only on surface runoff; and the requirement for a certain level of expertise to properly configure, parameterize, and interpret the results. Nevertheless, the results of this study clearly suggest that the proposed method can be effective in estimating design flows in ungauged catchments. Since the obtained results for the design flows may require adjustment, further research is needed to identify threshold values for catchment area, peak flows, and return periods at which such corrections should be made. Given that the method is intended for ungauged catchments, it is essential to determine the scaling coefficient values for corrections based on hydrological information from controlled catchments with similar characteristics. Future studies should also include assessing the impact of land use and catchment characteristics on the magnitude of estimation errors for the design flows. Nevertheless, the proposed DEFRAST approach is straightforward and effective, and it can serve as a tool for calculating design flows for infrastructure design in ungauged catchments.

Acknowledgments. This study was supported by an internship visit, of principal author Prof. Dariusz MłyŃski and author Prof. Andrzej Walega, hosted by USDA Forest Service Southern Research Station Santee Experimental Forest and a travel fund to both the authors by the grant of Rector of University of Agriculture in Krakow for April–June 2023 period. We are thankful for the rainfall and streamflow data provided by USDAFS researchers, Dr. John Campbell at the Hubbard Brook, Dr. Pete Caldwell at the Coweeta Hydrology Laboratory, and Charles A. Harrison at the Santee Experimental Forests. The opinions presented in this article are those of the authors and should not be construed to represent any official USDA or U.S. government determination or policy.

Data availability statement. All USDA-FS data used in this study can be available from the USDA Forest Service research data archive: Forest Service Research Data Archive (usda.gov). For Hubbard Brook sites, data also are accessed at Hubbard Brook Data Catalog—Hubbard Brook Ecosystem Study.

REFERENCES

Ajmal, M., M. Waseem, D. Kim, and T. W. Kim, 2020: A pragmatic slope-adjusted Curve Number Model to reduce uncertainty in predicting flood runoff from steep watersheds. *Water*, **12**, 1469, https://doi.org/10.3390/w12051469.

Ali, G. A., and A. G. Roy, 2010: A case study on the use of appropriate surrogates for antecedent moisture conditions (AMCs). *Hydrol. Earth Syst. Sci.*, **14**, 1843–1861, https://doi.org/10.5194/hess-14-1843-2010.

Ali, S., and A. Rahman, 2022: Development of a kriging-based regional flood frequency analysis technique for South-East Australia. *Nat. Hazards*, **114**, 2739–2765, https://doi.org/10.1007/s11069-022-05488-4.

Amatya, D. M., and A. Radecki-Pawlik, 2007: Flow dynamics of three experimental forested watersheds in coastal South Carolina (USA). *Acta Scientiarum Polonorum. Formatio Circumiectus*, **6**, 3–17.

——, S. Herbert, C. C. Trettin, and M. D. Hamidi, 2021a: Evaluation of paired watershed runoff relationships since recovery from a major hurricane on a coastal forest—A basis for examining effects of *Pinus palustris* restoration on water yield. *Water*, **13**, 3121, https://doi.org/10.3390/w13213121.

——, and Coauthors, 2021b: Estimates of precipitation IDF curves and design discharges for road-crossing drainage structures: Case study in four small forested watersheds in the southeastern US. *J. Hydrol. Eng.*, **26**, 05021004, https://doi.org/10.1061/(ASCE)HE.1943-5584.0002052.

——, A. Walega, T. J. Callahan, A. Morrison, V. Vulava, D. R. Hitchcock, T. M. Williams, and T. Epps, 2022: Storm event analysis of four forested catchments on the Atlantic coastal plain using a modified SCS-CN rainfall-runoff model. *J. Hydrol.*, **608**, 127772, https://doi.org/10.1016/j.jhydrol.2022.127772.

Anderegg, W. L. R., and Coauthors, 2020: Climate-driven risks to the climate mitigation potential of forests. *Science*, **368**, 6497, https://doi.org/10.1126/science.aaz7005.

Barnett, T. P., J. C. Adam, and D. P. Lettenmaier, 2005: Potential impacts of a warming climate on water availability in snow-dominated regions. *Nature*, **438**, 303–309, https://doi.org/10.1038/nature04141.

Bartlett, M. S., A. J. Parolari, J. J. McDonnell, and A. Porporato, 2016: Beyond the SCS-CN method: A theoretical framework for spatially lumped rainfall-runoff response. *Water Resour. Res.*, **52**, 4608–4627, https://doi.org/10.1002/2015WR018439.

Berthet, L., V. Andréassian, C. Perrin, and P. Javelle, 2009: How crucial is it to account for the antecedent moisture conditions in flood forecasting? Comparison of event-based and continuous approaches on 178 catchments. *Hydrol. Earth Syst. Sci.*, **13**, 819–831, https://doi.org/10.5194/hess-13-819-2009.

Bezak, N., M. Brillyc, and M. Šraj, 2016: Flood frequency analyses, statistical trends and seasonality analyses of discharge data: A case study of the Litija station on the Sava River. *J. Flood Risk Manage.*, **9**, 154–168, https://doi.org/10.1111/jfr3.12118.

Bhagat, N., 2017: Flood frequency analysis using Gumbel's distribution method: A case study of lower Mahi basin, India. *J. Water Res. Ocean Sci.*, **6**, 51–54, https://doi.org/10.11648/j.wros.20170604.11.

Caldwell, P. V., C. F. Miniat, K. J. Elliott, W. T. Swank, S. T. Brantley, and S. H. Laseter, 2016: Declining water yield from forested mountain watersheds in response to climate change and forest mesophication. *Global Change Biol.*, **22**, 2997–3012, https://doi.org/10.1111/gcb.13309.

Dai, Z., C. C. Trettin, and D. M. Amatya, 2013: Effects of climate variability on forest hydrology and carbon sequestration on the Santee experimental forest in coastal South Carolina. USDA Forest Service Southern Research Station, General Tech. Rep. SRS–172, 32 pp., https://www.srs.fs.usda.gov/pubs/gtr/gtr_srs172.pdf.

Elliott, K. J., P. V. Caldwell, S. T. Brantley, C. F. Miniat, J. M. Vose, and W. T. Swank, 2017: Water yield following forest–grass–forest transitions. *Hydrol. Earth Syst. Sci.*, **21**, 981–997, https://doi.org/10.5194/hess-21-981-2017.

Folton, N., E. Martin, P. Arnaud, P. L'Hermite, and M. Tolsa, 2019: A 50-year analysis of hydrological trends and processes in a Mediterranean catchment. *Hydrol. Earth Syst. Sci.*, **23**, 2699–2714, https://doi.org/10.5194/hess-23-2699-2019.

Green, W. H., and G. A. Ampt, 1911: Studies on soil phyics. *J. Agri. Sci.*, **4** (1), 1–24, https://doi.org/10.1017/S0021859600001441.

Green, M. B., S. W. Bailey, J. L. Campbell, K. J. McGuire, A. S. Bailey, T. J. Fahey, N. Lany, and D. Zietlow, 2021: A catchment water balance assessment of an abrupt shift in evapotranspiration at the Hubbard Brook Experimental Forest, New Hampshire, USA. *Hydrol. Processes*, **35**, e14300, https://doi.org/10.1002/hyp.14300.

Grimaldi, S., and A. Petroselli, 2015: Do we still need the rational formula? An alternative empirical procedure for peak discharge estimation in small and ungauged basins. *Hydrol. Sci. J.*, **60**, 67–77, https://doi.org/10.1080/02626667.2014.880546.

——, ——, and F. Serinaldi, 2012a: Design hydrograph estimation in small and ungauged watersheds: Continuous simulation method versus event-based approach. *Hydrol. Processes*, **26**, 3124–3134, https://doi.org/10.1002/hyp.8384.

——, ——, F. Tauro, and M. Porfiri, 2012b: Time of concentration: A paradox in modern hydrology. *Hydrol. Sci. J.*, **57**, 217–228, https://doi.org/10.1080/02626667.2011.644244.

——, ——, and N. Romano, 2013: Curve-number/Green–Ampt mixed procedure for streamflow predictions in ungauged basins: Parameter sensitivity analysis. *Hydrol. Processes*, **27**, 1265–1275, https://doi.org/10.1002/hyp.9749.

Hamed, K. H., and A. R. Rao, 1998: A modified Mann-Kendall trend test for autocorrelated data. *J. Hydrol.*, **204**, 182–196, https://doi.org/10.1016/S0022-1694(97)00125-X.

Hejduk, L., A. Hejduk, and K. Banasik, 2015: Determination of Curve Number for snowmelt-runoff floods in a small catchment. *Proc. IAHS*, **370**, 167–170, https://doi.org/10.5194/piahs-370-167-2015.

Hettiarachchi, S., C. Wasko, and A. Sharma, 2019: Can antecedent moisture conditions modulate the increase in flood risk due to climate change in urban catchments? *J. Hydrol.*, **571**, 11–20, https://doi.org/10.1016/j.jhydrol.2019.01.039.

Hossain, S., G. A. Hewa, and S. Wella-Hewage, 2019: A comparison of continuous and event-based Rainfall–Runoff (RR) modelling using EPA-SWMM. *Water*, **11**, 611, https://doi.org/10.3390/w11030611.

Houessou-Dossou, E. A. Y., J. M. Gathenya, M. Njugana, Z. A Gariy, and A. Petroselli, 2022: Comparative analysis of flood and rainfall frequency in the ungauged sub-watersheds of Kakia and Esamburumbur in Narok town, Kenya, using the EBA4SUB rainfall-runoff model. *J. Agric. Eng.*, **53**, 1307, https://doi.org/10.4081/jae.2022.1307.

Huang, X., Z. H. Shi, H. D. Zhu, H. Y. Zhang, L. Ai, and Y. Yin, 2016: Soil moisture dynamics within soil profiles and associated environmental controls. *Catena*, **136**, 189–196, https://doi.org/10.1016/j.catena.2015.01.014.

Kemp, D., and G. H. Alankarage, 2023: Benchmarking three event-based rainfall-runoff routing models on Australian catchment. *Hydrology*, **10**, 131, https://doi.org/10.3390/hydrology10060131.

Kuichling, E., 1889: The relation between the rainfall and the discharge of sewers in populous districts. *Trans. Amer. Soc. Civ. Eng.*, **20** (1), 1–56, https://doi.org/10.1061/TACEAT.0000694.

Laseter, S. H., C. R. Ford, J. M. Vose, and L. W. Swift Jr., 2012: Long-term temperature and precipitation trends at the Coweeta Hydrologic Laboratory, Otto, North Carolina, USA. *Hydrol. Res.*, **43**, 890–901, https://doi.org/10.2166/nh.2012.067.

Li, M., Q. Liu, H. Zhang, R. R. Wells, L. Wang, and J. Geng, 2022: Effects of antecedent soil moisture on rill erodibility and critical shear stress. *Catena*, **216**, 106356, https://doi.org/10.1016/j.catena.2022.106356.

Liu, B., D. Wang, S. Fu, and W. Cao, 2017: Estimation of peak flow rates for small drainage areas. *Water Resour. Manage.*, **31**, 1635–1647, https://doi.org/10.1007/s11269-017-1604-y.

Liu, N., P. V. Caldwell, G. R. Dobbs, C. F. Miniat, P. V. Bolstad, S. A. C. Nelson, and G. Sun, 2021: Forested lands dominate drinking water supply in the conterminous United States. *Environ. Res. Lett.*, **16**, 084008, https://doi.org/10.1088/1748-9326/ac09b0.

Mateo-Lázaro, J., J. Castillo-Mateo, J. Á. Sánchez-Navarro, V. Fuertes-Rodríguez, A. García-Gil, and V. Edo-Romero, 2019: Assessment of the role of snowmelt in a flood event in a gauged catchment. *Water*, **11**, 506, https://doi.org/10.3390/w11030506.

Merz, B., and Coauthors, 2022: Understanding heavy tails of flood peak distributions. *Water Resour. Res.*, **58**, e2021WR030506, https://doi.org/10.1029/2021WR030506.

Miniat, C. F., and Coauthors, 2021: The Coweeta Hydrologic Laboratory and the Coweeta LTER Project. *Hydrol. Processes*, **35**, e14302, https://doi.org/10.1002/hyp.14302.

Młyński, D., A. Petroselli, and A. Wałęga, 2018: Flood frequency analysis by an event-based rainfall-runoff model in selected catchments of southern Poland. *Soil and Water Research*, **13**, 170–176, https://doi.org/10.17221/153/2017-SWR.

Młyński, D., A. Wałęga, T. Stachura, and G. Kaczor, 2019: A new empirical approach to calculating flood frequency in ungauged catchments: A case study of the Upper Vistula Basin, Poland. *Water*, **11**, 601, https://doi.org/10.3390/w11030601.

——, ——, B. Ozga-Zieliński, M. Ciupak, and A. Petroselli, 2020: New approach for determining the quantiles of maximum annual flows in ungauged catchments using the EBA4SUB model. *J. Hydrol.*, **589**, 125198, https://doi.org/10.1016/j.jhydrol.2020.125198.

Mukherjee, S., and Coauthors, 2024: A watershed-scale multi-approach assessment of design flood discharge estimates used in hydrologic risk analyses for forest road stream crossings and culverts. *J. Hydrol.*, **632**, 130698, https://doi.org/10.1016/j.jhydrol.2024.130698.

——, and Coauthors, 2025: Hydro-geomorphological assessment of culvert vulnerability to flood-induced soil erosion using an ensemble modeling approach. *J. Environ. Modell. Software*, **183**, 106243, https://doi.org/10.1016/j.envsoft.2024.106243.

Petroselli, A., 2020: A generalization of the EBA4SUB rainfall–runoff model considering surface and subsurface flow. *Hydrol. Sci. J.*, **65**, 2390–2401, https://doi.org/10.1080/02626667.2020.1810856.

——, S. Asgharinia, T. Sabzevari, and B. Saghafian, 2019a: Comparison of design peak flow estimation methods for ungauged basins in Iran. *Hydrol. Sci. J.*, **65**, 127–137, https://doi.org/10.1080/02626667.2019.1686506.

——, S. Grimaldi, R. Piscopia, and F. Tauro, 2019b: Design hydrograph estimation in small and ungauged basins: A comparative assessment of event based (EBA4SUB) and continuous (COSMO4SUB) modeling approaches. *Acta Sci. Pol. Form. Circimiectus*, **18**, 113–124, https://doi.org/10.15576/ASP.FC/2019.18.4.113.

Petroselli , A., E. Arcangeletti, E. Allegrini, R. Nunzio, and S. Grimaldi, 2013: The influence of the net rainfall mixed Curve Number – Green Amptprocedure in flood hazard mapping: a case study in Central Italy. *Journal of Agricultural Engineering*, **44**, 58–61.

Piscopia, R., A. Petroselli, and S. Grimaldi, 2015: A software package for predicting design-flood hydrographs in small and ungauged basins. *J. Agric. Eng.*, **46**, 74–84, https://doi.org/10.4081/jae.2015.432.

Radevski, I., S. Gorin, O. Dimitrovska, I. Milevski, B. Apostolovska-Toshevska, M. Talevska, and V. Zlatanoski, 2016: Estimation of maximum annual discharges by frequency analysis with four probability distributions in case of non-homogeneous time series (Kazani karst spring in Republic of Macedonia). *Acta Carsologica*, **45**, 253–262, https://doi.org/10.3986/ac.v45i3.1544.

Recanatesi, F., and A. Petroselli, 2020: Land Cover Change and flood risk in a peri-urban environment of the Metropolitan area of Rome (Italy). *Water Resour. Manage.*, **34**, 4399–4413, https://doi.org/10.1007/s11269-020-02567-8.

Shi, W., and N. Wang, 2020: An improved SCS-CN method incorporating slope, soil moisture, and storm duration factors for runoff prediction. *Water*, **12**, 1335, https://doi.org/10.3390/w12051335.

Swank, W. T., and D. A. Crossley, Jr., 1988: Introduction and site description. *Forest Hydrology and Ecology at Coweeta*, W. T. Swank and D. A. Crossley, Eds., Ecological Studies, Vol. 66, Springer, 3–16.

Trettin, C. C., D. M. Amatya, A. Muwamba, J. Glover, and R. Wenerick, 2021: Ecoregion 8.5.3 southern coastal plain: Santee experimental forest, South Carolina. Biological responses to stream nutrients: A synthesis of science from experimental forests and ranges, General Tech. Rep. PNW-GTR-981, 389–414, https://www.fs.usda.gov/pnw/pubs/pnw_gtr981_chapter15.pdf.

USDA–NRCS, 2010: Time of concentration. *National Engineering Handbook (NEH) Part 630*, U.S. Department of Agriculture Natural Resources Conservation Service, 15i–15B–3, https://www.hydrocad.net/neh/630ch15.pdf.

USDA, 1986: Urban hydrology for small watersheds. USDA Tech. Release 55, 164 pp.

Vojtek, M., A. Petroselli, J. Vojteková, and S. Asgharinia, 2019: Flood inundation mapping in small and ungauged basins: Sensitivity analysis using the EBA4SUB and HEC-RAS modeling approach. *Hydrol. Res.*, **50**, 1002–1019, https://doi.org/10.2166/nh.2019.163.

Wałęga, A., 2016: The importance of calibration parameters on the accuracy of the floods description in the Snyder's model. *J. Water Land Dev.*, **28**, 19–25, https://doi.org/10.1515/jwld-2016-0002.

——, and D. M. Amatya, 2020: Application of modified SME-CN method for predicting event runoff and peak discharge from a drained forest watershed on the North Carolina Atlantic coastal plain. *Trans. ASABE*, **63**, 275–288, https://doi.org/10.13031/trans.13838.

——, ——, P. Caldwell, D. Marion, and S. Panda, 2020: Assessment of storm direct runoff and peak flow rates using improved SCS-CN models for selected forested watersheds in the Southeastern United States. *J. Hydrol. Reg. Stud.*, **27**, 100645, https://doi.org/10.1016/j.ejrh.2019.100645.

Wasko, C., R. Nathan, and M. C. Peel, 2020: Changes in antecedent soil moisture modulate flood seasonality in a changing climate. *Water Resour. Res.*, **56**, e2019WR026300, https://doi.org/10.1029/2019WR026300.

Yerswa, B. T., and M. B. Chane, 2024: Regional climate models and bias correction methods for rainfall-runoff modeling in Katar watershed, Ethiopia. *Environ. Syst. Res.*, **13**, 10, https://doi.org/10.1186/s40068-024-00340-z.